

# Interfacial Behavior of Epichlorohydrin–Ethyleneoxide–Allylglycidyl Ether/Fluorinated Carbon Black Observed from Mechanical and Dielectrical Properties

A. Katada, T. Shimura, Y. Tominaga, S. Asai, M. Sumita

Department of Chemistry and Materials Science, Tokyo Institute of Technology, 2-12-1 Ookayama, Meguro-Ku, Tokyo 152-8552, Japan

Received 14 May 2003; accepted 8 July 2003

**ABSTRACT:** The purpose of this work was to study the effect of carbon black (CB) surface state on the interaction between CB and polymer matrix, as well as the polymer chain mobility. The mobility of polymer chain absorbed on the CB surface was estimated by using a dynamic mechanical analyzer and an impedance analyzer. The interaction parameter ( $B$ ) and immobilized polymer layer thickness ( $\Delta R$ ) were estimated from the dynamic mechanical analysis. It was observed that values of  $B$  and  $\Delta R$  decreased with increasing fluorine content on the CB surface. On the other hand, from the dielectric measurement, the Maxwell–Wagner–Sillars (MWS) relaxation peak, accompanied by migration of the charge carriers, accumulated at the interface between polymer and CB, observed at temperatures higher

than the glass-transition temperature ( $T_g$ ) of the polymer matrix. The activation energy ( $E_{a,MWS}$ ), calculated from the relaxation frequency of MWS relaxation, was decreased with increasing surface fluorine content. Good agreement was found between the  $B$  and the  $\Delta R$  values estimated from the dynamic mechanical analysis and the  $E_{a,MWS}$  calculated from the MWS relaxation frequency estimated from dielectric measurement. © 2004 Wiley Periodicals, Inc. *J Appl Polym Sci* 91: 2928–2933, 2004

**Key words:** fluorinated carbon black; epichlorohydrin–ethyleneoxide–allylglycidyl ether; dynamic mechanical property; MWS relaxation; chain; mobility

## INTRODUCTION

It is known that the physical properties of composites consisting of polymer matrix and carbon black (CB) particles greatly depend not only on the volume fraction of CB particles but also on the surface state of CB particles. For example, the dispersion state of surface-treated CB particles in the matrix composed of immiscible polymer blends was found to be affected by the interfacial free energy calculated from the surface energy of polymer matrix and CB particles.<sup>1,2</sup> Moreover, the activation energy calculated from the dynamic percolation, which is a dynamic process to form a conductive path in the CB-filled polymer composite at high temperature (greater than the melting point of the matrix polymer), increases with increasing surface energy of CB particles.<sup>3,4</sup> Besides, the bound rubber thickness estimated from <sup>1</sup>H-NMR of the composite of natural rubber (NR)/oxidized CB particles is lower than that of NR/untreated CB particles.<sup>5,6</sup>

With respect to surface fluorination, it has been established that the treatment of surface fluorination of particles causes a decrease of surface energy.<sup>7–10</sup>

Concerning the physics of poly(vinylidene fluoride) and surface fluorinated carbon black (FCB) composite, the percolation curve gradually becomes less pronounced by surface fluorine treatment.<sup>10</sup> Moreover, the mixing torque of the composite consists of styrene–butadiene–rubber (SBR) and fluorinated carbon black decreased with increasing fluorine content,<sup>7</sup> which is attributed to the weakened interaction by surface fluorine treatment. Thus, the FCB is expected as a new class of reinforcing or conducting filler. However, the effect of mobility of polymer chain on FCB particles is not yet clear.

With this in mind, the dynamic mechanical analysis (DMA) measurement with CB-filled polymer composite is an effective tool for determining the interaction between polymer matrix and filler particles. In particular, the interaction parameter ( $B$ ) and the immobilized polymer layer thickness ( $\Delta R$ ) calculated from DMA measurement<sup>11–13</sup> have been used to obtain information about the interaction between the polymer matrix and filler surface.

Furthermore, it is known that the dielectric analysis of polymer composite material shows Maxwell–Wagner–Sillars (MWS)<sup>14–16</sup> relaxations under certain conditions. The origin of MWS relaxation is accompanied by the migration of charge carriers that accumulated at the polymer–filler interface. The activation energy calculated from the MWS relaxation frequency for the

Correspondence to: M. Sumita (msumita@o.cc.titech.ac.jp).

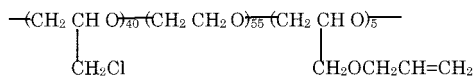


Figure 1 Molecular structure of CHR.

composites made of polymer matrix and more conductive filler depends not only on the respective values of the conductivities and permittivities but also on the shape and size of the fillers.<sup>16,17</sup> However, the relationship between the MWS relaxation and the mobility of polymer chain on filler surface is not yet clear, given that it is very difficult to separate the peak of MWS relaxation and  $\alpha$ -relaxation of the polymer matrix.<sup>18–20</sup>

In this study, we investigated the interfacial interaction between polymer and the surface of CB particles, prepared by FCB particles in semiconductive epichlorohydrin–ethyleneoxide–allylglycidyl ether (CHR) matrix by DMA measurement. At the same time, we also studied the relationship between the MWS relaxation behavior in the dielectric measurement and the interfacial interaction between CHR and FCB particles.

## EXPERIMENTAL

### Materials and sample preparation

The polymer matrix, epichlorohydrin–ethyleneoxide–allylglycidyl ether (CHR), was supplied by Nihon Zeon Co. (Japan). The density of CHR was 1.10 g cm<sup>-3</sup>. The molecular structure of CHR is shown in Figure 1. The weight-average molecular weight ( $M_w$ ), number-average molecular weight ( $M_n$ ), and  $M_w/M_n$  of CHR determined by gel permeation chromatography (GPC) were  $1.672 \times 10^6$ ,  $8.105 \times 10^5$ , and 2.063, respectively. The glass-transition temperature ( $T_g$ ), measured by differential scanning calorimetry (DSC) under a heating rate of 20°C/min, was -48°C.

Three kinds of carbon black particles (CB0, FCB010, FCB025) with different F/C atomic ratios of 0, 0.10, and 0.25 supplied by Daikin Industries Co. (Japan) were used as fillers. The density of these FCB powders was 1.95 g cm<sup>-3</sup>. The F/C atomic ratios were estimated from elemental analysis.<sup>21,22</sup> The fluorinated

CB (FCB) particles were synthesized by the direct fluorination of CB0 at about 400°C.<sup>21,22</sup> The physical characteristics of CB particles are summarized in Table I. We assumed that the diameter of various FCB particles did not change with increasing F/C atomic ratio. The Brunauer–Emmett–Teller (BET)<sup>23</sup> surface area increased with increasing F/C atomic ratio. On the other hand, the London dispersive component of surface energy ( $\gamma^d$ ) decreased with increasing F/C atomic ratio.

In this work, the CB0, FCB010, and FCB025 particles were dried at 110°C for 24 h under vacuum before mixing with CHR. The mechanical mixing process was performed using a two-roll mixer for 30 min at 60°C. The freestanding sheets (1.0 mm thickness) were obtained from the mixtures using compression molding at 60°C for 10 min under a pressure of 19.6 MPa.

### Dynamic mechanical property

Dynamic mechanical analysis was used for the quantitative estimation of rubber–filler interaction by comparing the  $\tan \delta$  value of the filled sample with that of the unfilled sample. It was carried out with IT-DVA 200s (ITK Co., Japan). For this measurement, the prepared freestanding sheets were cut into rectangular specimens (30 × 5 mm). The experiment was performed in a tension mode with 0.1% strain amplitude at a frequency of 3.5 Hz. The temperature ranged from -50 to -20°C with a heating rate of 5°C/min.

### Dielectric property

The composite molded freestanding sheets (20 mm<sup>2</sup>) were cut from the center part of the molded sample sheet and were fixed on a glass plate with copper film as electrode using a polyimide tape. The prepared cell was then placed in a temperature-controlled chamber. The nitrogen gas was used to prevent the samples from oxidation during measurements. The complex permittivity ( $\epsilon^*$ ), the real-part permittivity ( $\epsilon'$ ), the imaginary loss factor ( $\epsilon''$ ), and the dissipation factor  $\tan \delta$  ( $\tan \delta = \epsilon''/\epsilon'$ ) were measured by a complex impedance method using a 4192A LF impedance analyzer (Hewlett–Packard, Palo Alto, CA) in the fre-

TABLE I  
Characteristics of Fluorinated Carbon Black Particles

Sample	F/C atomic ratio	Diameter (nm)	Surface area (m <sup>2</sup> /g) <sup>a</sup>	Surface energy, $\gamma^d$ (mJ/m <sup>2</sup> ) <sup>a</sup>
CB0	0.0	42	47.9	126
FCB010	0.10	42	57.0	121
FCB025	0.25	42	68.1	99

<sup>a</sup> Measured by inverse gas chromatography (IGC); probe *n*-octane (C<sub>8</sub>), column temperature: 110°C.

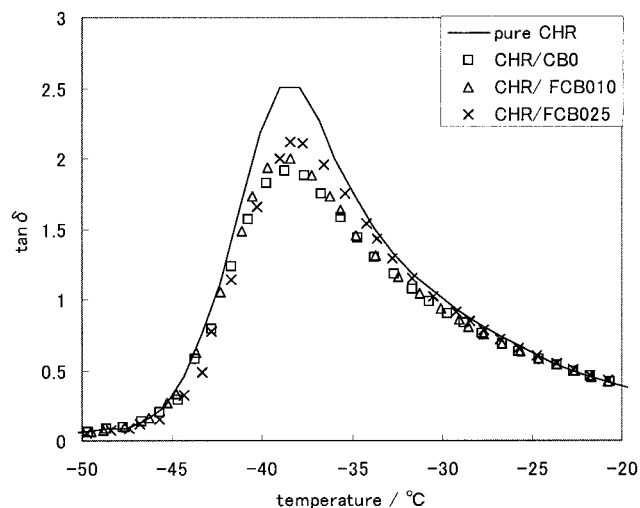


**Figure 2** Tan  $\delta$  versus temperature for pure CHR (solid line) and CHR composite containing 6 vol % CB0 ( $\square$ ), FCB010 ( $\Delta$ ), and FCB025 ( $\times$ ).

quency range from 0.01 kHz to 10 MHz. The temperature was varied from  $-70$  to  $150^\circ\text{C}$  with a heating rate of  $2^\circ\text{C}/\text{min}$ .

## RESULTS AND DISCUSSION

### Dynamic mechanical property

Figure 2 shows the temperature dependency of  $\tan \delta$  of pure CHR and the CHR composites containing 6 vol % CB0, FCB010, and FCB025. The  $\tan \delta$  was calculated from the ratio  $E''/E'$ , which is the ratio of energy loss per cycle to the maximum energy stored per cycle. It is known that  $E''$  is related to the dissipation energy by heating attributed to the deformation of the material and the  $E'$  is a measure of recoverable strain energy in the deformed material. As shown in Figure 2, a peak at around  $-38^\circ\text{C}$  attributed to the glass-rubber transition of CHR matrix was observed. It was seen that the  $\tan \delta$  at glass-transition temperature was decreased by the addition of CB particles. With respect to molecular motion, it is thought that some of the CHR molecules in the CB0 composite are absorbed preferentially and form bound rubber, which greatly constrains the molecular motions of the CHR chain, resulting in the decrease of  $\tan \delta$ . Among the CB-filled polymer composites, the  $\tan \delta$  slightly increased with increasing F/C atomic ratio of CB particles.

In the present work, dynamic mechanical studies were used for the quantitative analysis of the extent of rubber-filler interaction by comparing the  $\tan \delta$  of filled and unfilled systems. If there was a significant physicochemical or specific interaction attributed to the London dispersive force or Lewis acid-base force between matrix rubber and filler particles, the interaction would tend to immobilize a layer of matrix rubber

around filler particles. Assuming the immobilized rubber chain around CB particles to be sufficiently rigid, the immobilized rubber layer will contribute to the effective filler volume fraction in the composite. As a result of such rubber-filler interaction, the interaction parameter  $B$  and the immobilized polymer layer thickness  $\Delta R$  were calculated from the following equation proposed by Ziegel,<sup>11</sup> Nielsen,<sup>12</sup> and Iisaka and Shibayama<sup>13</sup>:

$$\frac{\tan \delta_c}{\tan \delta_r} = 1 - B\phi_f \quad (1)$$

where  $\phi_f$  is the volume fraction of filler and subscripts  $c$  and  $r$  refer to the composite and pure rubber, respectively. In particular, this equation is useful to the region around the  $T_g$  of matrix polymer for DMA measurement. The interaction parameter  $B$ , which presents the extent of rubber-filler interaction, is related to the effective thickness of the matrix rubber-filler interface.

$$B = (1 + \Delta R/R)^3 \quad (2)$$

where  $R$  is the radius of fillers and  $\Delta R$  is the apparent thickness of the immobilized polymer layer. Table II shows the values of  $\tan \delta$ ,  $B$ , and  $\Delta R$  for the CHR composites containing a 6 vol % CB0, FCB010, and FCB025. These  $B$  and  $\Delta R$  values were calculated from eqs. (1) and (2). As shown in Table II, these  $B$  and  $\Delta R$  values decreased with increasing F/C atomic ratio. In other words, the reduction of the dispersive component of surface energy ( $\gamma^d$ ) caused the weak interaction between the polymer matrix and CB particles. Such a tendency—the decrease of  $B$  and  $\Delta R$  with the decrease of  $\gamma^d$  of CB particles—was also observed in general rubbers [natural rubber (NR), styrene-butadiene-rubber (SBR), and acrylonitrile-butadiene-rubber (NBR)] filled with alkylated silica.<sup>24,25</sup>

### Dielectric property

In general, it is known that the charge carriers accumulate at the interface when an electrical voltage was applied to the composite consisting of two compo-

**TABLE II**  
Values of  $\tan \delta$ , Interaction Parameter ( $B$ ), and Immobilized Polymer Layer ( $\Delta R$ ) for CB0-filled, FCB010-filled, and FCB025-filled CHR

Sample	$\tan \delta$	$B$	$\Delta R$ (nm)
Pure CHR	2.50	—	—
CHR/CB0	1.92	3.87	12.1
CHR/FCB010	2.00	3.33	10.5
CHR/FCB025	2.12	2.53	7.9

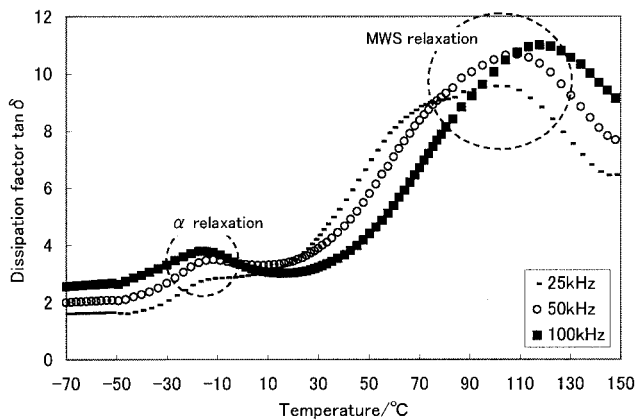


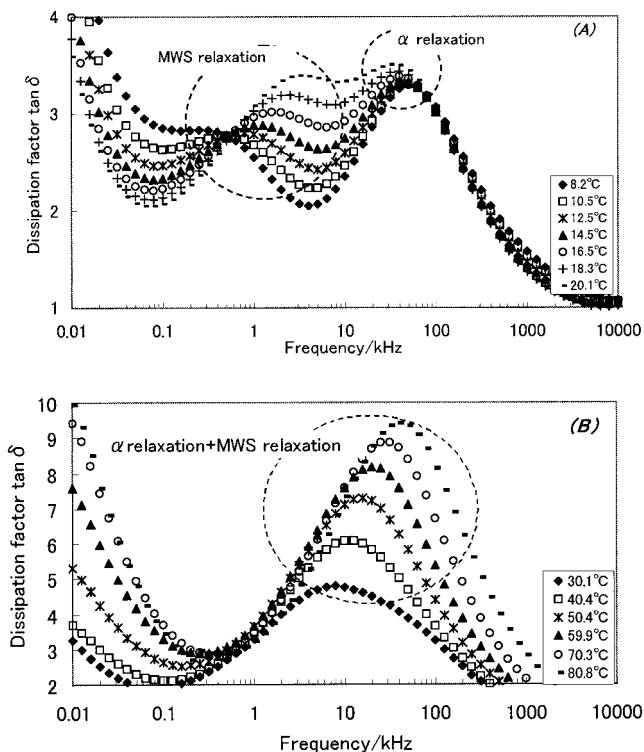
**Figure 3** Temperature dispersion of dissipation factor  $\tan \delta$  for CHR composite containing 14 vol % CB0 as a function of measurement frequency; —: 25 kHz; ○: 50 kHz; ■: 100 kHz.

nents that have different permittivities and conductivities. This effect is called as Maxwell–Wagner–Sillars (MWS) effect.<sup>14–16</sup>

In this system, for the composites made of a polymer matrix in which inclusions of a more conductive material are embedded, the charge carriers accumulate at the interface of the polymer and the inclusions. It seems reasonable to suppose that the charge carriers can migrate by the relaxation of the polymer chain at the interface between the polymer matrix and the CB particles.

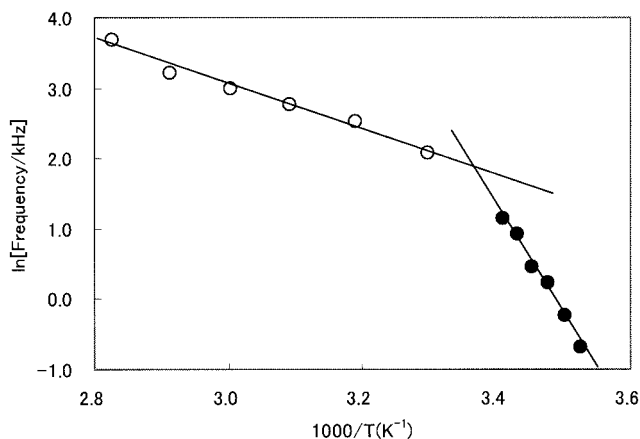
Figure 3 shows the temperature dispersion of the dissipation factor  $\tan \delta$  in the temperature range from  $-70$  to  $150^\circ\text{C}$  for the CHR composite containing 14 vol % CB0 as a function of measurement frequency. Two  $\tan \delta$  peaks can be observed in Figure 3. The low-temperature peaks are assigned to the  $\alpha$ -relaxation process, and the high-temperature peaks are assigned to the MWS relaxation process. The  $\alpha$ -relaxation process is associated with the segmental motion by the glass–rubber transition process. Meanwhile, the MWS relaxation process is associated with the migration of the charge carriers accompanied by the relaxation of the immobilized polymer chain on the CB surface. In experimental results, the peak temperature of  $\tan \delta$  for the  $\alpha$ -relaxation is slightly dependent on the frequency. On the other hand, the peak temperature of  $\tan \delta$  for MWS relaxation has a significant relationship with the frequency. It has been reported that the MWS relaxation temperature is about  $100^\circ\text{C}$  higher than that of  $\alpha$ -relaxation.<sup>19,20</sup>

Figure 4(A) and (B) show the relationships between dissipation factor  $\tan \delta$  and frequency for CHR composite containing 14 vol % CB0. Figure 4(A) and (B) show the low-temperature region ( $8$ – $20^\circ\text{C}$ ) and the high temperature region ( $30$ – $80^\circ\text{C}$ ), respectively. In almost every case, it is difficult to separate the MWS and  $\alpha$ -relaxation processes from each other.<sup>19,20</sup> Therefore many research-



**Figure 4** Dissipation factor  $\tan \delta$  versus frequency for CHR composite containing 14 vol % CB0: (A) low-temperature region ( $8$ – $20^\circ\text{C}$ ); (B) high-temperature region ( $30$ – $80^\circ\text{C}$ ).

ers have regarded the peak composed of MWS and  $\alpha$ -relaxation processes as the peak of MWS relaxation process. The double peak can be seen in the frequency dispersion of dissipation factor  $\tan \delta$  as shown in Figure 4(A), where it is shown that the peak in the higher-frequency region ( $\sim 100$  kHz) is attributed to the  $\alpha$ -relaxation process, and the peak in the frequency region ranging on the order of about 1 kHz is attributed to the MWS relaxation process.<sup>17–20,26</sup> The information derived



**Figure 5** Arrhenius plot of the maximum frequency of dissipation factor  $\tan \delta$  for MWS relaxation versus reciprocal temperature for CHR composite containing 14 vol % CB0.

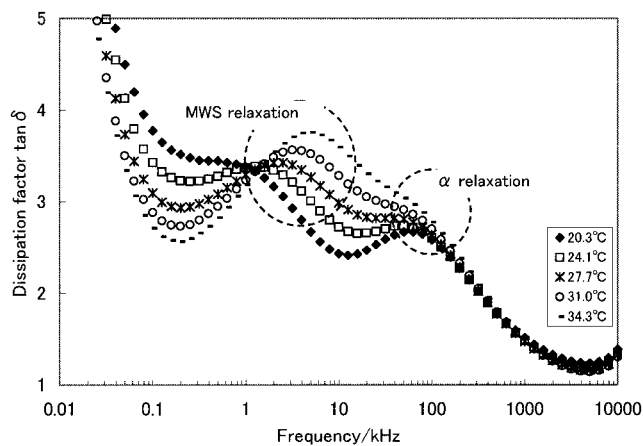


**Figure 6** Dissipation factor  $\tan \delta$  versus frequency for CHR composite containing 18 vol % FCB010.

from Figure 4(A) is helpful for strictly estimating the molecular mobility on the carbon black surface. To identify this relaxation, the plot of the frequencies, at which the  $\tan \delta$  maximum appears, versus reciprocal temperatures of the experiment are presented in Figure 5. The filled circle in Figure 5 was estimated from the pure MWS relaxation process in Figure 4(A), although the open circle in Figure 5 was estimated from the relaxation process consisting of MWS and  $\alpha$ -relaxation in Figure 4(B). The activation energy ( $E_a$ ) of the filled circle ( $E_{aMWS}$ ) is 131 kJ/mol, and the activation energy of the open circle ( $E_{aMWS+\alpha}$ ) is 26 kJ/mol. These values were calculated from an Arrhenius equation  $f = f_0 \exp(-E_a/kT)$ , where  $f$  is the frequency of  $\tan \delta$  maximum,  $k$  is the Boltzmann constant, and  $T$  is the absolute temperature. In this study, we will discuss the relationship between the  $E_a$  calculated from the frequency of  $\tan \delta$  maximum for the pure MWS relaxation and the interfacial interaction of CHR and FCB particles.

Figures 6 and 7 give the frequency dispersion of dissipation factor  $\tan \delta$  as a function of measurement

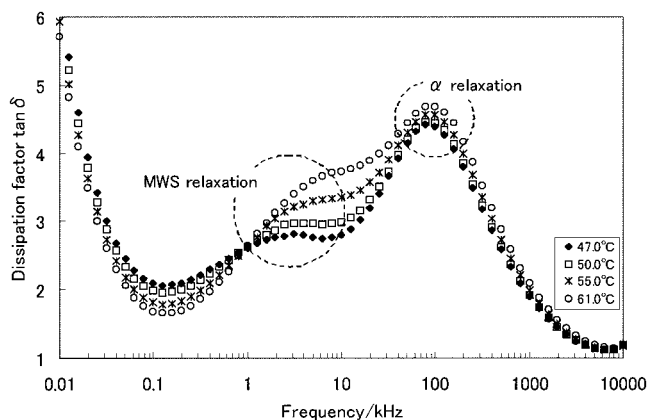


**Figure 7** Dissipation factor  $\tan \delta$  versus frequency for CHR composite containing 27 vol % FCB025.

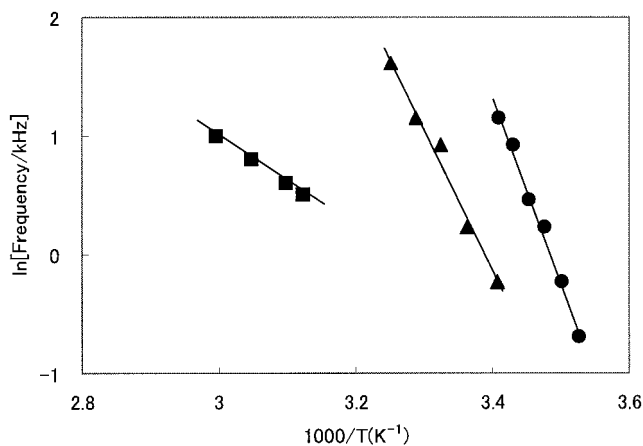


**Figure 8** Arrhenius plots of the maximum frequency of dissipation factor  $\tan \delta$  for MWS relaxation versus reciprocal temperature for FCB-loaded CHRs. ●: CB0-filled CHR; ▲: FCB010-filled CHR; ■: FCB025-filled CHR.

temperature for CHR composite containing 18 vol % FCB010 and containing 27 vol % FCB025, respectively. Two peaks of  $\tan \delta$ , which are assigned to MWS and  $\alpha$ -relaxation processes, can be seen in the frequency dispersion in these figures as well as in Figure 4(A). Figure 8 shows the Arrhenius plots of  $\tan \delta$  maximum for MWS relaxation of CHR composites containing 14 vol % CB0 (filled circle), 18 vol % FCB010 (filled triangle), and 27 vol % FCB025 (filled square), respectively. The values of activation energy of MWS relaxation,  $E_{aMWS}$ , calculated from an Arrhenius equation are listed in Table III for three samples of CHR composites. It has been suggested that  $E_{aMWS}$  values do not depend on filler content.<sup>18,19</sup> We point out that the  $E_{aMWS}$  decreases with increasing fluorine content on the CB surface. The reduction of the  $\gamma^d$  by fluorine modification promotes the weak interaction between CHR and CB particles. As a result, the constraint on the CHR rubber matrix relatively decreased. Therefore, charge carriers on the CB surface can easily migrate. This result coincides with the result that the  $B$  and  $\Delta R$  values decrease with increasing fluorine content of the CB surface (see Table II).

## CONCLUSIONS

Dynamic mechanical analysis (DMA) and dielectric analysis were conducted on a series of epichlorohy-

**TABLE III**  
Activation Energies ( $E_{aMWS}$ ) Estimated from the Pure MWS Relaxation Frequency

Sample	$E_{aMWS}$ (kJ/mol)
CHR/CB0	131
CHR/FCB010	99
CHR/FCB025	75

drin-ethyleneoxide-allylglycidyl ether (CHR) matrices filled with surface-fluorinated carbon black particles of different fluorine content: 0 (CB0), 0.10 (FCB010), and 0.25 (FCB025).

From DMA, the interaction parameter ( $B$ ) and the immobilized polymer layer thickness ( $\Delta R$ ) were evaluated from the  $\tan \delta$  peak at the glass-transition temperature of the CHR matrix. Values of  $B$  and  $\Delta R$  decreased with increasing fluorine content of CB particles.

From the dielectric analysis, two peaks of  $\tan \delta$  could be seen in the frequency dispersion, which are assigned to MWS and  $\alpha$ -relaxation processes. The activation energy ( $E_{a\text{MWS}}$ ) of the pure MWS relaxation process decreased with increasing surface fluorine content, which is attributed to the fluorine treatment to the CB surface that weakened interfacial interaction between CHR and CB particles. It was found that the result of pure MWS relaxation measured by an impedance analyzer is relevant to the interfacial interaction between the polymer matrix and the filler particles.

## References

1. Asai, S.; Sakata, K.; Sumita, M.; Miyasaka, K. *Polym J* 1992, 24, 415.
2. Wu, S.; Asai, S.; Sumita, M. *Sen-i-Gakkaishi* 1993, 49, 103 (in Japanese).
3. Asai, S.; Sumita, M. *J Macromol Sci Phys* 1995, B34, 283.
4. Wu, G.; Asai, S.; Zhang, C.; Miura, T.; Sumita, M. *J Appl Phys D Appl Phys* 2000, 88, 1480.
5. Asai, S.; Kaneki, H.; Sumita, M.; Miyasaka, K. *J Appl Polym Sci* 1991, 43, 1253.
6. Serizawa, H.; Nakamura, T.; Ito, M.; Tanaka, K.; Nomura, A. *Polym J* 1983, 3, 201.
7. Rodriguez, J.; Hamed, G. R. *Rubber Chem Technol* 1996, 69, 286.
8. Nakahara, M.; Ozawa, K.; Sanada, Y. *J Mater Sci* 1994, 29, 1614.
9. Setoyama, N.; Li, G.; Kaneko, K. *Adsorption* 1996, 2, 293.
10. Wu, G.; Zhang, C.; Miura, T.; Asai, S.; Sumita, M. *J Appl Polym Sci* 2000, 80, 1063.
11. Ziegel, K. D. *Colloid Interface Sci* 1969, 29, 72.
12. Nielsen, L. E. *J Polym Sci Part B: Polym Phys* 1979, 18, 1897.
13. Iisaka, K.; Shibayama, K. *J Appl Polym Sci* 1978, 22, 3135.
14. Maxwell, K. W. *Electricity and Magnetism, Vol. 1*; Clarendon: Oxford, UK, 1982.
15. Wagner, K. W. *Arch Electrotechnol (Berl)* 1914, 2, 37.
16. Sillars, R. W. *J Inst Elect Eng* 1937, 80, 378.
17. Van Beek, L. K. H. *Prog Dielectrics* 1967, 7, 69.
18. Aldrich, P. D.; McGee, R. L.; Yalvac, S.; Bonekamp, J. E.; Thurrow, S. W. *J Appl Phys* 1987, 62, 4504.
19. Perrier, G.; Bergeret, A. *J Appl Phys* 1995, 77, 2651.
20. Perrier, G.; Bergeret, A. *J Polym Sci Part B: Polym Phys* 1997, 35, 1349.
21. Isogai, T.; Maruyama, S.; Yamana, M.; Kubo, M. Abstracts of the 21st Annual Meetings of The Carbon Society (Japan), 1994; abstr. 278.
22. Isogai, T.; Kawashima, T.; Uehara, H.; Maruyama, S.; Yamaguchi, F.; Kubo, M.; Hattri, Y.; Touhara, H. Abstracts of the International Symposium on Carbon, 1998; abstr. 24.
23. Brunauer, S.; Emmet, P. H.; Teller, J. *J Am Chem Soc* 1938, 60, 309.
24. Ou, Y. C.; Yu, Z. Z.; Vidal, A.; Donnet, J. B. *Rubber Chem Technol* 1994, 67, 834.
25. Ou, Y. C.; Yu, Z. Z.; Vidal, A.; Donnet, J. B. *J Appl Polym Sci* 1996, 59, 1321.
26. Banhegyi, G. *Colloid Polym Sci* 1988, 266, 11.